Environmental Science & Technology

Article

pubs.acs.org/est

High Levels of Daytime Molecular Chlorine and Nitryl Chloride at a Rural Site on the North China Plain

Xiaoxi Liu,[†] Hang Qu,[†] L. Gregory Huey,[*,†] Yuhang Wang,[*,†] Steven Sjostedt,[†,‡,§] Limin Zeng,[∥] Keding Lu,[∥] Yusheng Wu,[∥] Min Hu,[∥] Min Shao,[∥] Tong Zhu,[∥] and Yuanhang Zhang[∥]

[†]School of Earth and Atmospheric Sciences, Georgia Institute of Technology, Atlanta, Georgia 30332, United States

[‡]Cooperative Institute for Research in Environmental Sciences, University of Colorado, Boulder, Boulder, Colorado 80309, United States

[§]Earth System Research Laboratory, National Oceanic and Atmospheric Administration, Boulder, Colorado 80305, United States

[∥]State Key Joint Laboratory of Environmental Simulation and Pollution Control, College of Environmental Sciences and Engineering, Peking University, Beijing 100871, China

Supporting Information

ABSTRACT: Molecular chlorine (Cl_2) and nitryl chloride ($ClNO_2$) concentrations were measured using chemical ionization mass spectrometry at a rural site over the North China Plain during June 2014. High levels of daytime Cl_2 up to ~450 pptv were observed. The average diurnal Cl_2 mixing ratios showed a maximum around noon at ~100 pptv. $ClNO_2$ exhibited a strong diurnal variation with early morning maxima reaching ppbv levels and afternoon minima sustained above 60 pptv. A moderate correlation (R^2 = 0.31) between Cl_2 and sulfur dioxide was observed, perhaps indicating a role for power plant emissions in the generation of the observed chlorine. We also observed a strong correlation (R^2 = 0.83) between daytime (10:00–20:00) Cl_2 and $ClNO_2$, which implies that both of them were formed from a similar mechanism. In addition, Cl_2 production is likely associated with a photochemical mechanism as Cl_2 concentrations varied with ozone (O_3) levels. The impact of Cl_2 and $ClNO_2$ as Cl atom sources is investigated using a photochemical box model. We estimated that the produced Cl atoms oxidized slightly more alkanes than OH radicals and enhanced the daily concentrations of peroxy radicals by 15% and the O_3 production rate by 19%.

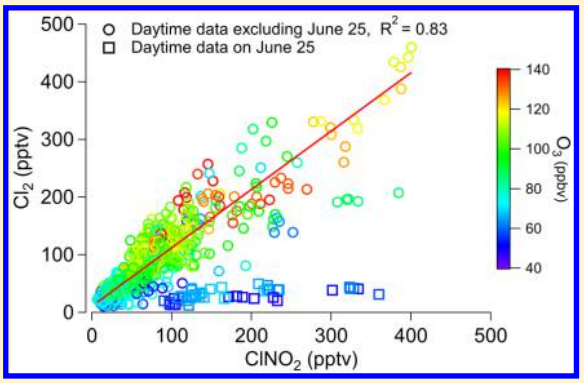

INTRODUCTION

Hydroxyl radicals (OH) are the primary oxidant in the daytime troposphere.[1,2] Chlorine atoms (Cl) can also act as oxidants by reacting with volatile organic compounds (VOCs). The chemistry of Cl atoms and OH radicals are different, as Cl atoms react up to 2 orders of magnitude faster with some VOCs (e.g., CH_4 and ethane) than OH.[3] Recent studies of chlorine atom precursors, such as molecular chlorine (Cl_2) and nitryl chloride ($ClNO_2$), indicate that chlorine chemistry in the troposphere is widespread.[4−7]

In the lower atmosphere, Cl_2 can be produced through autocatalytic halogen activation and photochemical processes.[8−12] Specifically, hypochlorous acid (HOCl) formed from the reaction of chlorine monoxide (ClO) and hydroperoxyl radical (HO_2) or chlorine nitrate ($ClONO_2$) formed from that of ClO and nitrogen dioxide (NO_2) can deposit to heterogeneous surfaces and react with chloride to produce Cl_2 (reactions 1−5).[11,12]

$$Cl + O_3 \rightarrow ClO + O_2 \quad (1)$$

$$ClO + HO_2 \rightarrow HOCl + O_2 \quad (2)$$

$$ClO + NO_2 + M \rightarrow ClONO_2 + M \quad (3)$$

$$HOCl + Cl^-(aq) + H^+(aq) \rightarrow Cl_2 + H_2O \quad (4)$$

$$ClONO_2 + Cl^-(aq) + H^+(aq) \rightarrow Cl_2 + HNO_3 \quad (5)$$

In addition, laboratory experiments, model simulations, and field observations in the Arctic imply that Cl_2 can form from the photolysis of O_3 in aqueous sea-salt particles or on saline snowpack or ice surfaces.[4,8,10] Cl_2 can also be directly emitted from industrial processes, such as power generation, oil and metal refining, and bleaching processes at water treatment plants.[13] A few studies have observed up to ~30 pptv Cl_2 in the daytime and up to ~200 pptv at night in polluted coastal marine boundary layer.[6,14−18] Liao et al. measured high levels of Cl_2, up to ~400 ppt during the day, in the lower Arctic atmosphere.[4] More recently, evidence for extensive chlorine radical chemistry

Received: June 13, 2017
Revised: August 7, 2017
Accepted: August 14, 2017
Published: August 14, 2017

DOI: 10.1021/acs.est.7b03039
Environ. Sci. Technol. 2017, 51, 9588−9595

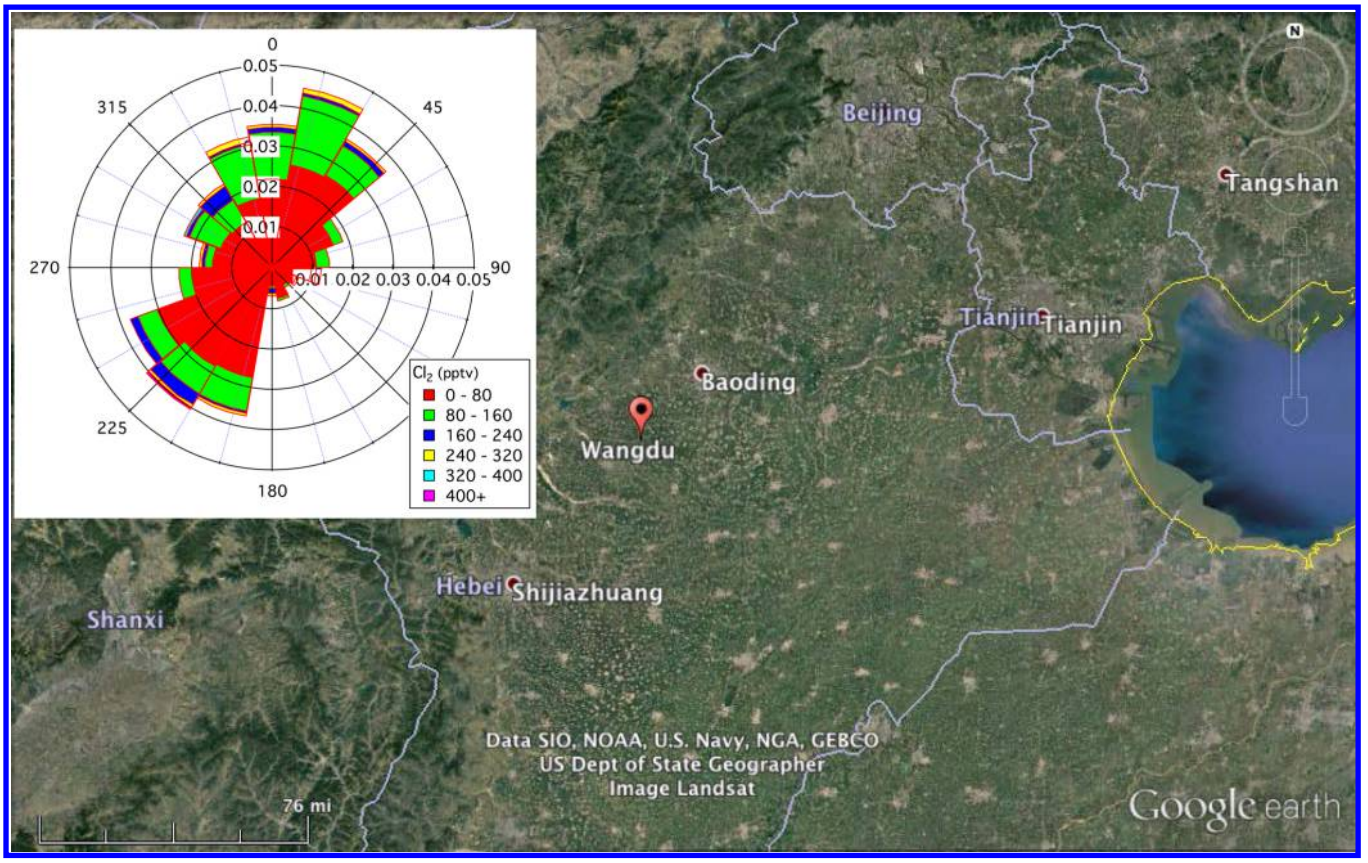

Figure 1. Location of Wangdu and surrounding provinces and major cities. The inset shows a wind rose showing frequency distribution of Cl_2 concentrations with legend indicating color code for each size bin in pptv.

associated with Asian pollution outflow was observed from aircraft over the Malaysian Peninsula in winter.[19] However, the mechanisms of chlorine production in these studies are not yet fully understood.

$ClNO_2$ can be produced from the reaction of dinitrogen pentoxide (N_2O_5) on chloride-containing aerosols.[20] In general, $ClNO_2$ accumulates during the night and photolyzes rapidly after sunrise to produce NO_2 and Cl atoms. $ClNO_2$ production is generally more efficient in polluted coastal regions due to abundant sea-salt aerosol and urban NO_x emissions. Recent studies observed up to ~5 ppbv of nighttime $ClNO_2$ in these regions.[6,7,21,22] $ClNO_2$ production also occurs inland where continental chloride is available from inland sources such as salt beds, coal combustion, and water treatment processes. Observations in continental air have revealed up to ~450 pptv nighttime or early morning $ClNO_2$.[5,18]

Observed Cl_2 and $ClNO_2$ levels suggest that chlorine chemistry can have a significant influence on oxidation chemistry. For example, in the Arctic boundary layer chlorine atoms can be a more important oxidant for methane than hydroxyl radicals.[4] Cl atoms formed by photolysis of 1.5 ppbv $ClNO_2$, contributed to net O_3 production of ~12 ppbv per day in Los Angeles according to a model simulation.[23] Nevertheless, due to limited direct measurements, the distribution and sources of reactive chlorine species remain unclear in many regions. It is therefore difficult to assess their impacts on photochemistry. Field measurements of Cl atom precursors have been mainly conducted in North America and Europe. In Asia, $ClNO_2$ measurements have been conducted only in Hong Kong while no Cl_2 measurements are available.[21] In addition, one concurrent study of Cl_2 and $ClNO_2$ is limited to the Los Angeles region, which limits a direct comparison of their relative importance in other regions.[6] Concurrent measurements of Cl species will also provide constraints on the mechanisms of reactive Cl cycling.

The North China Plain (NCP) region, including several provinces and megacities such as Beijing and Tianjin, suffers from severe air pollution events and frequent haze.[24,25] In June and July 2014, the Campaigns of Air Pollution Research in Megacity Beijing and North China Plain (CAREBEIJING-NCP) was conducted in Wangdu, Hebei Province (38.665°N, 115.204°E), which is 170 km southwest of Beijing on the NCP (Figure 1). The measurement site was surrounded by over a dozen of coal-fired power plants within 200 km and was also impacted by residential coal combustion for cooking and agricultural activities such as crop residue burning and fertilization (e.g., Figures 1 and S1 in Tham et al.).[26,27] The main objective of this campaign was to understand radical chemistry and oxidative processes in the NCP region. Tham et al. have already presented a detailed assessment of nighttime and early morning $ClNO_2$ observations and relevant chemistry, but they had few observations in daytime.[26] In this work, we primarily focus on the surprising observations of daytime (i.e., 10:00−20:00) $ClNO_2$ and Cl_2. The potential sources of these species are investigated and the impact of Cl_2 and $ClNO_2$ as Cl atom sources is also assessed with a photochemical box model.

METHODS

A chemical ionization mass spectrometer (CIMS) was deployed during the CAREBEIJING-NCP study from June 11 to July 8 2014. The I^--CIMS instrument used to detect chlorine species

DOI: 10.1021/acs.est.7b03039
Environ. Sci. Technol. 2017, 51, 9588−9595

was very similar to that we have used to measure Cl_2, bromine oxide, and peroxyacetyl nitrate (PAN).[4,28,29] Ambient air was delivered to the CIMS through a perfluoroalkoxy (PFA) Teflon tubing, with dimensions of ~4 m length, 1/2″ outer diameter, and 3/8″ inner diameter. The portion of the inlet that extended out of the window was wrapped with aluminum foil to prevent exposure to sunlight. The opening of the sampling inlet was at ~6 m above the ground. A total flow of ~4.5 standard liters per minute (slpm) was sampled. A portion of this flow, 1.2 slpm, was sampled into the last ~45 cm of inlet tubing and then entered the CIMS, with the rest exhausted. The total residence time in the sampling line was less than 4 s. In addition, an oven was installed at the final 15 cm of inlet tubing in front of the flow tube orifice, essentially identical to the inlet configuration used previously to measure PAN.[28] A critical orifice with a diameter of 0.4 mm was placed before the oven, which lowered the pressure inside the oven to ~120 Torr. This greatly reduced possible interference to PAN from NO, as NO can react with the thermally generated peroxyacetyl radical. The measurements automatically switched between heated cycles, with the oven heated to 170 °C, and ambient-temperature cycles every 30 min. Iodide (I^-) was used as the reagent ion. Cl_2 and $ClNO_2$ were detected as cluster ions ICl_2^- and $IClNO_2^-$, respectively. They also produce Cl^- at the same time by reacting with I^- (reactions 6–9). At a study-averaged water vapor concentration of 23 parts per thousand by volume, the lab-determined ratios of ICl_2^- to Cl^- and $IClNO_2^-$ to Cl^- are 1:1.2 and 1:1.1, respectively.

$$Cl_2 + I^- \rightarrow ICl_2^- \quad (6)$$

$$Cl_2 + I^- \rightarrow Cl^- \quad (7)$$

$$ClNO_2 + I^- \rightarrow IClNO_2^- \quad (8)$$

$$ClNO_2 + I^- \rightarrow Cl^- \quad (9)$$

Cl_2 and $ClNO_2$ were only quantified during the cool cycles of the oven, since heating the inlet likely resulted in aerosol evaporation and thus potential interferences to Cl_2 and $ClNO_2$. Specifically, increases in ICl_2^- signals were observed with the oven on while the $ClNO_2$ slightly decreased. The backgrounds of Cl_2 and $ClNO_2$ were determined by scrubbing the ambient sample with a charcoal and glass wool filter, while that of PAN was determined by the addition of ~3 ppmv NO to destroy the detected peroxyacetyl radicals. On-site calibration was performed by adding a known amount of PAN to the inlet from a photolytic source twice every heated cycle.[30] The relative sensitivities of Cl_2 and $ClNO_2$ to that of PAN were determined in the laboratory after the campaign as a function of water vapor concentrations as encountered during the campaign (Figure S1 of the SI).[18,28] A Cl_2 permeation tube (KIN-TEK Laboratories, Inc.) was used to calibrate the sensitivity of Cl_2. The emission rate of the permeation tube was quantified by bubbling the effluent through a buffered potassium iodide solution that converted the Cl_2 quantitatively to triiodide (I_3^-), which was then measured by UV absorption at 352 nm. $ClNO_2$ was generated by passing a humidified flow of Cl_2 in N_2 over a bed of sodium nitrite ($NaNO_2$).[18,31] $ClNO_2$ was then delivered simultaneously to the CIMS and a NO_2 monitor (Aerodyne Research, Inc.) using cavity attenuated phase shift spectroscopy.[32] The CIMS sensitivity of $ClNO_2$ was then determined by dissociating $ClNO_2$ to NO_2 in a quartz inlet with temperatures ranging from 285 to 375 °C and measuring the increase in NO_2 concentrations and the decrease in $IClNO_2^-$ signals.

The natural isotopic abundances of ^{35}Cl and ^{37}Cl are 75.76% and 24.24%, respectively.[33] Cl species were measured at m/z = 197 and 199 for ICl_2^-, m/z = 208 and 210 for $IClNO_2^-$, and m/z = 35 and 37 for Cl^-. By plotting the 5 min averaged ambient raw signal (background signal subtracted) at these pairs of masses (Figure S2), we found good correlations with R^2 ranging from 0.83 to 0.99. In addition, the observed ratios of m/z = 199 vs 197 (0.58 ± 0.01), m/z = 210 vs 208 (0.3113 ± 0.0003), and m/z = 37 vs 35 (0.2859 ± 0.0004) are very close to the ratios due to natural Cl isotopes (0.640 ± 0.003, 0.320 ± 0.001, and 0.320 ± 0.001). In addition, no systematic variation in day and night ratios was seen. These results indicate that species containing one or two Cl atoms are detected at these masses at ambient temperatures. However, since there are small discrepancies between the ideal and the observed ratios, it is important to note that the possibility of unknown positive interference in these measurements cannot be ruled out. This is especially true, as this location consistently yielded the most complicated I^- mass spectra that we have observed (e.g., Figure S3). Chlorine isotope fractionation during the multiphase cycling of Cl could also perturb the ideal isotope ratio by a few parts per thousand.[34,35]

Elevated daytime (10:00–20:00) Cl^- signals at m/z = 35 and 37 that matched expected isotopic ratio of Cl (Figure S2c) were observed during the campaign. A major source of the daytime (10:00–20:00) Cl^- signals was Cl_2 through reaction 7, as 47% of the variation in Cl^- signals could be explained by the linear relationship between ICl_2^- and Cl^- signals (Figure S2d). The remaining variance could be partially explained by the variation in ambient water vapor concentrations, as higher water vapor favored reaction 6 over reaction 7.[18] The presence of other Cl-containing gases such as HOCl, ClO, chlorine nitrate ($ClONO_2$), and $ClNO_2$ (R^2 = 0.16) could also generate Cl^- ions. In addition, the variance of instrumental background signals could also degrade the ICl_2^- and Cl^- correlation.

Previous studies have shown that inlet artifacts for $ClNO_2$ including generation and loss were usually negligible.[5,6] As for the observed Cl_2, it is unlikely that it resulted from the conversion of HOCl, $ClONO_2$, or $ClNO_2$ on the inlet surface. Liao et al. estimated an upper limit of the HOCl conversion to Cl_2 on an NaCl-coated version of our inlet of 15%.[4] Although reaction 5 is certainly possible on our inlet walls, the ambient $ClONO_2$ produced at our current inferred Cl atom levels (Figure S7) would be smaller than needed to produce our measured Cl_2 concentrations. If the observed Cl_2 were from HOCl or $ClONO_2$ conversion, this would imply very large daytime concentrations of ClO and thus even more Cl atoms in this region. In previous work using a similar inlet, we measured $ClNO_2$ and Cl_2 using CIMS in Atlanta, Georgia, U.S.A. in winter (December 2012 to March 2013, Figure S13) and summer (July 2015), respectively. $ClNO_2$ in winter ranged from below detection limit to ~480 pptv, while there was essentially no $ClNO_2$ observed in summer. In both seasons, Cl_2 levels in Atlanta were always below or near our limit of detection and showed no correlation with elevated $ClNO_2$. Thus, we concluded that the observed Cl_2 at Wangdu was not an artifact from $ClNO_2$. The transmission efficiency of Cl_2 through the inlet was assumed to be unity. This was confirmed by field tests in Atlanta, which showed that Cl_2 loss onto the inlet wall was negligible for an identical inlet with the same flow conditions. However, wall loss of Cl_2 cannot be completely ruled out in Wangdu since the inlet could be coated by pollutants, which were not simulated in Atlanta. Despite this, the good correlations between isotopes support the existence of large quantities of Cl_2 and $ClNO_2$ and potentially other chlorine

DOI: 10.1021/acs.est.7b03039
Environ. Sci. Technol. 2017, 51, 9588–9595

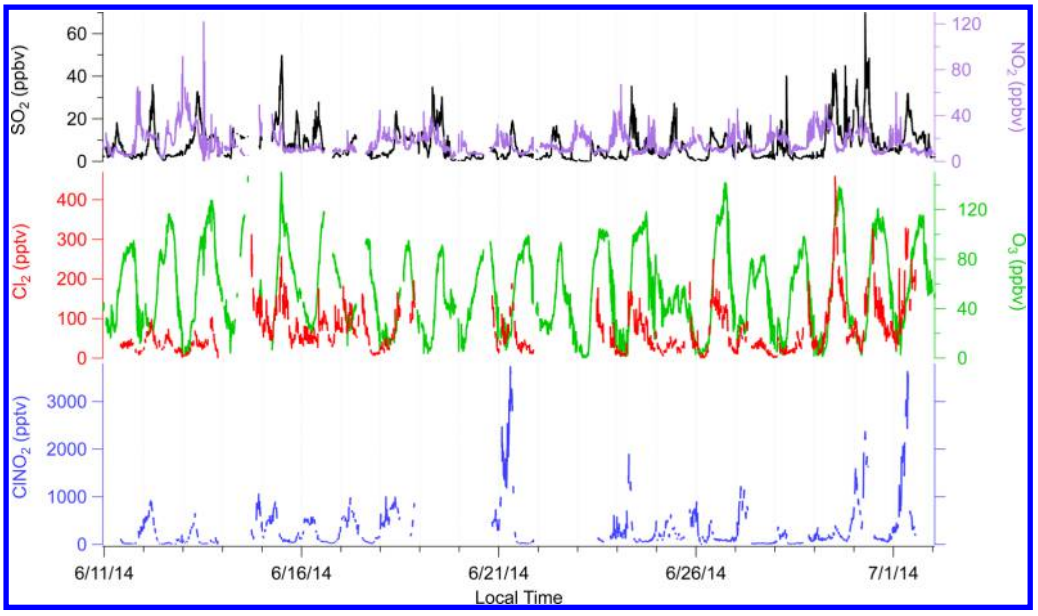

Figure 2. Time series of 5 min averaged $ClNO_2$ and Cl_2 and 1 min SO_2, NO_2, and O_3. The vertical grid indicates midnight in Beijing time.

species in the NCP region. Finally, it is worth noting that wall loss of Cl_2 will only lead to an underestimation of its concentration in this study.

We estimated the overall measurement uncertainties to be 30% for PAN, 33% for Cl_2, and 36% for $ClNO_2$. The overall 30% uncertainty in PAN resulted from combining 5% for standard NO gas, 13% for 1σ of PAN calibration signals, and an estimated 27% for the NO-to-PAN conversion efficiency of the PAN calibration source. The total uncertainty in Cl_2 includes an additional 4% for the Cl_2 permeation rate and 12% in the Cl_2 to PAN sensitivity ratio. Besides these, $ClNO_2$ uncertainties were associated with 10% for the accuracy of the NO_2 monitor and 10% for the $ClNO_2$ to Cl_2 sensitivity ratio. The campaign-averaged sensitivities of PAN (hot), Cl_2 (cool), and $ClNO_2$ (cool) are 2.3 ± 1.6, 1.0 ± 0.7, and 1.3 ± 0.9 Hz/pptv. The detection limits of PAN, Cl_2, and $ClNO_2$ measurements are estimated to be 8, 7, and 3 pptv (a signal-to-noise ratio of 2) for 1 min data. Here we report the measurements of Cl_2 and $ClNO_2$ from June 11 to July 1 when the CIMS and the PAN calibration source were under relatively good condition despite frequent power outages.

A suite of gas and aerosol measurements were also utilized in this work.[26] A 0-D box model was used to assess the impact of Cl atoms released from Cl_2 and $ClNO_2$. The box model was based on the 1-D version of the Regional chEmical trAnsport Model and was updated with known Cl chemistry.[36−38] The model was constrained by the observed Cl_2, $ClNO_2$, and other available species and photolysis frequencies. A detailed description of the model and a complete list of relevant measurements and techniques can be found in the Supporting Information.

RESULTS AND DISCUSSION

Figure 2 shows a time series of Cl_2, $ClNO_2$, O_3, SO_2, and NO_2 from June 11 to July 1 2014. Cl_2 and $ClNO_2$ are shown as 5 min averages when the inlet was at ambient temperature. Data gaps in Cl_2 and $ClNO_2$ longer than ∼1 h were primarily due to power outages and occasionally due to instrument maintenance. Cl_2 mixing ratios during this period ranged from below detection limit to ∼450 ppt. High levels of Cl_2 over 100 pptv were observed on 16 out of 19 days when measurements were available. Among the existing Cl_2 observations, only the Cl_2 levels observed at Barrow, Alaska are comparable to those observed at Wangdu.[4] Figure 3 shows an average diurnal pattern of Cl_2. The average Cl_2

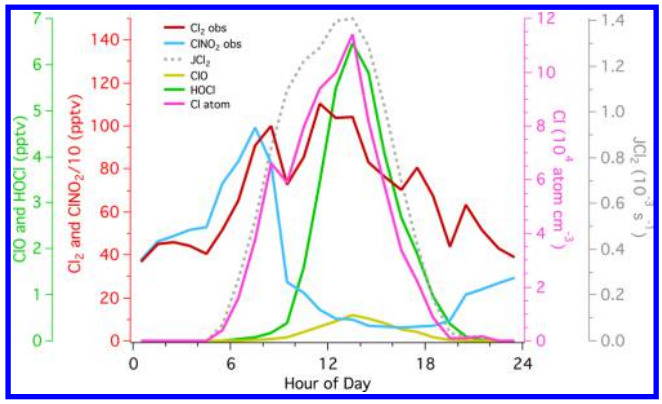

Figure 3. Average diurnal profiles of observed Cl_2 and $ClNO_2$ and model-predicted JCl_2, ClO, HOCl, and Cl atoms from June 11 to July 1.

mixing ratios were relatively low during the night and ranged between 30 and 50 pptv. Cl_2 began to increase at around 05:00, reaching the daytime peak by 11:00−14:00, with an average concentration slightly larger than 100 pptv. Cl_2 levels then decreased through the afternoon.

Elevated $ClNO_2$ was detected every night during the measurement period. The several highest levels occurred on the mornings of June 21 (∼3740 pptv), July 1 (∼3640 pptv), and June 30 (∼2380 pptv). The lowest nighttime/early morning $ClNO_2$ was observed on June 28−29, with the highest peaks less than 400 pptv. Our $ClNO_2$ measurements overlapped with those conducted by Tham et al. on the nights of June 21, 24−25, 28−30, and July 1.[26] In addition to the overlapping period, our measurements between June 11 and 18 and on June 26 and 27 complement $ClNO_2$ data in this region and showed consistent $ClNO_2$ accumulation reaching ppbv levels in the early morning. The average $ClNO_2$ diurnal profile (Figure 3) shows a typical nighttime accumulation and a following increase in concentrations after sunrise at ∼04:50. $ClNO_2$ peaked around 07:00−

DOI: 10.1021/acs.est.7b03039
Environ. Sci. Technol. 2017, 51, 9588−9595

08:00 and decreased through the morning. Surprisingly, average $ClNO_2$ levels sustained above 60 pptv in the afternoon despite a short photolysis lifetime of ~35 min around noon. Such an afternoon level cannot be explained by daytime N_2O_5 reactive uptake. Morning peaks after sunrise have also been observed by Tham et al. at Wangdu, Bannan et al. in London U.K., and Faxon et al. in Texas, U.S.A.[26,39,40] At Wangdu, the cause has been speculated by Tham et al. as mixing with $ClNO_2$-rich air mass from upper levels shortly after sunrise.[26]

Given the short photolysis lifetime of Cl_2 during the day (~8 min at noon), the observation of high levels implies that there must have a significant daytime source. To obtain insight into the source of Cl_2, we examined the relationship between Cl_2 and meteorological conditions and local pollutants. During the period of June 11 to July 1 2013, the winds were predominantly southwesterly, northeasterly, and northerly. It is likely that the Wangdu site was affected by urban plumes from nearby cities, such as Baoding and Tianjin to the northeast and Shijiazhuang to the southwest. In order to determine if Cl_2 had a local source or was distributed regionally, we plotted a wind rose graph examining all measured Cl_2 as a function of wind direction (Figure 1). Relatively high Cl_2 levels (>80 pptv) were generally associated with the dominant wind directions, but there was no systematic enhancement from a particular direction. This also applies to daytime Cl_2 (Figure S5). The two-day transport history of air masses shows a predominantly continental origin for air masses during the study. Most of the air mass trajectories were southerly. In other cases, June 23 and June 27−28 were characterized by northeasterly and northerly trajectories, respectively. June 12−14 and June 20−21 were two periods of easterly trajectories originating over the Bohai Sea and passing by the megacity Tianjin, corresponding to moderate Cl_2 levels up to ~190 pptv. So there is likely a significant continental source of Cl_2 precursors since it was regularly observed in continental air masses with no coastal influence.

For 30 min averaged data, we found weak correlation between Cl_2 and observations of the mobile source tracer, NO_x (R^2 = 0.01), and a biomass burning tracer, potassium ion (R^2 = 0.004). Cl_2 is only weekly correlated with observed HCl (R^2 = 0.08) and particulate chloride (R^2 = 0.01). In contrast, a better correlation between Cl_2 and SO_2 was found with R^2 = 0.31. Except for the Cl_2-potassium relationship (in which case p = 0.11), all the p-values of these correlations are less than 0.05, which indicates that the corresponding regression coefficients are statistically significant. As also can be seen from Figure 2, Cl_2 and SO_2 peaks often, however not always, occurred at a similar time. Since SO_2 was mainly emitted by power plants, this may imply that power plant emissions may be a source of Cl_2 precursors.[41]

We also investigated the relationship between 5 min Cl_2 and $ClNO_2$ throughout the measurement period. Their relationship varied at night (Figure S6). Various reasons could be responsible for the nighttime variation, such as different production processes and loss rates and the transport of air masses to the measurement site with different portions of Cl_2 and $ClNO_2$. In contrast, due to rapid loss by photolysis, the observed daytime Cl_2 and $ClNO_2$ were more likely produced locally than affected by transport. A strong correlation between daytime Cl_2 and $ClNO_2$ (between 10:00 and 20:00, R^2 = 0.83) was observed for all days when O_3 levels were moderate or high (Figure 4). This implies that both Cl_2 and $ClNO_2$ were formed by a similar mechanism during the day, though the exact mechanism remains unclear. The June 25 data followed a different trend line with a significantly smaller slope than the other days. On June 25 due to

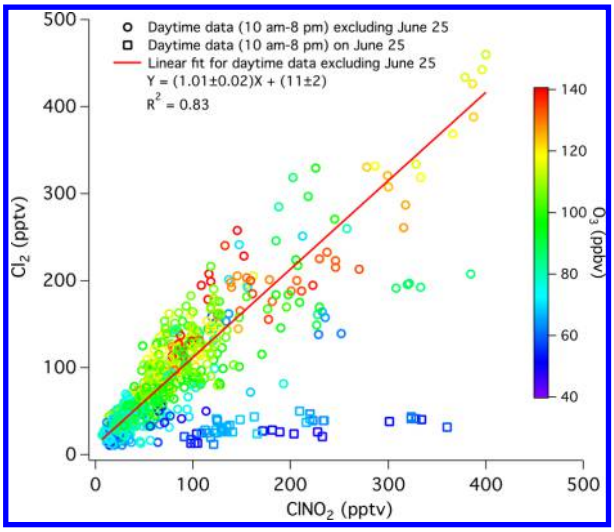

Figure 4. Scatter plot of 5 min Cl_2 versus $ClNO_2$ between 10 am and 8 pm colored by O_3 concentrations. Circles represent all daytime data excluding June 25 and squares represent daytime data on June 25. Results of orthogonal distance regression are shown.

attenuated solar radiation, the levels of O_3 and OH, measured by laser-induced fluorescence, were also the lowest during the studied period with noontime peaks less than 60 ppbv (Figure 2) and 2×10^6 molecules cm^{-3}, respectively.[42] Thus, we suspect that daytime Cl_2 production involved photochemistry or photochemical produced products so that Cl_2 production was less significant when O_3 concentration was low.

Two possible explanations for the correlation between daytime Cl_2 and $ClNO_2$ were explored. First, some daytime $ClNO_2$ can be produced by the reaction of Cl + NO_2 (reaction 10) with the Cl atoms generated from Cl_2 photolysis. To determine whether this was the case, the photochemical model simulated $ClNO_2$ produced by this reaction and lost by photolysis using the amount of Cl atoms originated from Cl_2, measured NO_2, and simulated photolysis rates. On average, reaction 10 can only generate a small fraction of the observed $ClNO_2$ (<~8%; Figure S8). Cl + NO_2 also produces chlorine nitrite (ClONO, reaction 11). Due to its more rapid photolysis, the generated ClONO is expected to be less than 6 pptv throughout the day (Figure S8). Even if ClONO reacts with I^- ions to produce $ICl NO_2^-$ cluster at m/z = 208, which is likely less efficient than reaction 8, the sum of simulated $ClNO_2$ and ClONO is still less than ~12% of the observed $ClNO_2$ levels during the day.[7] However, if Cl_2 was lost in the inlet at Wangdu, the measured ratio of $Cl_2/ClNO_2$ is too low, and a larger fraction of the $ClNO_2$ could be explained by the presence of Cl_2. Second, Roberts et al. proposed based on laboratory experiments that the reaction of $ClNO_2$ with aerosol phase chloride yields Cl_2 at pH ≤2.[43] We used a thermodynamic equilibrium model, ISORROPIA-II, to predict $PM_{2.5}$ pH by constraining to the measured SO_4^{2-}−NO_3^-−NH_4^+−Na^+−Cl^-−K^+−HNO_3−NH_3−HCl system.[44,45] The study average ± standard deviation $PM_{2.5}$ pH is 3.9 ± 1.1 (Figure S10). During the studied period, the pH was almost always >2, except for June 27 afternoon (as low as 1.1) and June 30 afternoon (as low as 1.8). Thus, for most of the time examined in this study, the particle pH was not estimated to be low enough to support this mechanism. In addition, the ratios of Cl_2 to $ClNO_2$ in Figure 4 cannot be simply explained by pH (Figure S11). Therefore, the correlation between daytime Cl_2 and $ClNO_2$ may result from other unknown mechanisms. Note

DOI: 10.1021/acs.est.7b03039
Environ. Sci. Technol. 2017, 51, 9588−9595

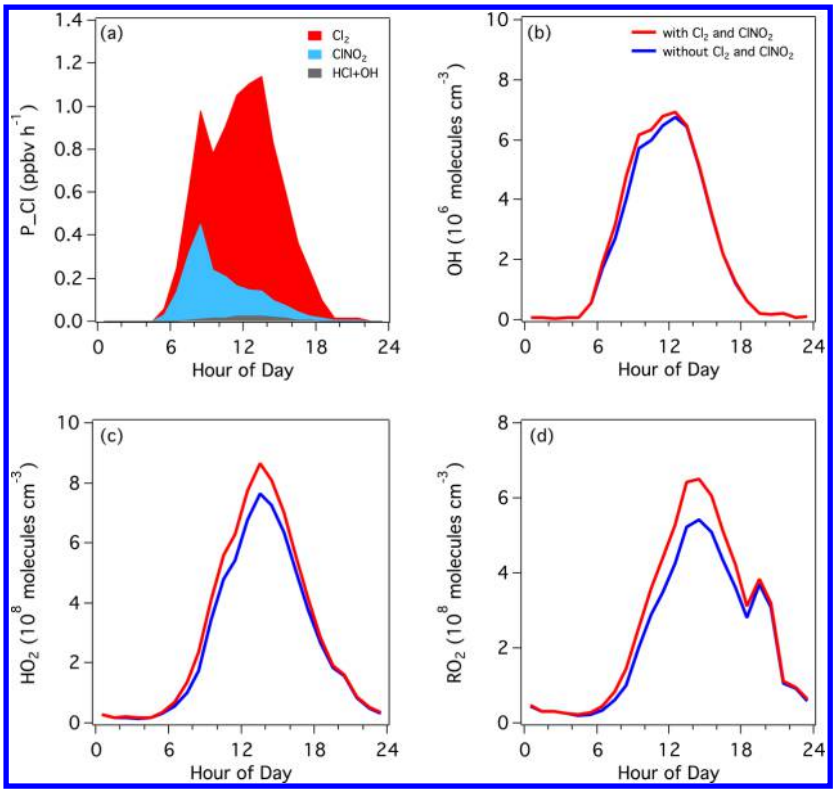

Figure 5. Modeled average radical profiles: (a) Cl atom production rate resulting from the photolysis of Cl_2 and $ClNO_2$ and the reaction of HCl + OH, (b) OH, (c) HO_2, and (d) RO_2. The red and blue lines represent results with and without initial inputs of Cl_2 and $ClNO_2$.

that we assumed no compositional dependence on particle size and treated the measured chemical constituents as bulk $PM_{2.5}$ properties (see SI for details). So it is possible that some smaller particles were more acidic than the model prediction.[46,47] Further investigation is needed to identify the sources of daytime Cl_2 and $ClNO_2$ in this region.

$$Cl + NO_2 + M \rightarrow ClNO_2 + M \quad (10)$$

$$Cl + NO_2 + M \rightarrow ClONO + M \quad (11)$$

The importance of Cl_2 and $ClNO_2$ as Cl atom sources is assessed using the box model. The average calculated Cl atom production rates from the photolysis of Cl_2 and $ClNO_2$ and the reaction of HCl + OH are shown in Figure 5. The total Cl atom production peaked at ~1 ppbv h^{-1} between 08:00−09:00 and 11:00−14:00, corresponding to the highest average levels of $ClNO_2$ and Cl_2 as shown in Figure 3. Cl_2 remains the major Cl atom source throughout the day and contributes 77% of the daily total production rate. As expected, the maximum $ClNO_2$ contribution to Cl atom production occurred in the early morning and reached 0.44 ppbv h^{-1}. $ClNO_2$ contributed to 21% of the integrated production rate during the day. The reaction of HCl plus OH only accounted for 2% of the daily production. Based on known chlorine chemistry (Table S2), the simulated average diurnal profiles of Cl, ClO, and HOCl are also plotted in Figure 3. Around noon, the predicted Cl atom reached 1.1×10^5 atoms cm^{-3}, which is about 1−2% of the noontime OH abundance. HOCl and ClO had similar profiles and peaked between 13:00 and 14:00 at 6.5 and 0.56 pptv, respectively.

The Cl atoms produced from the observed Cl_2 and $ClNO_2$ can significantly contribute to VOC oxidation at this location. Using the model simulated Cl atom and OH concentrations, we compared the effect of Cl atoms on the measured VOCs. When averaged to a daily basis, 16% of methane, 55% of other alkanes, 8% of alkenes, and 7% of aromatics were oxidized by Cl atoms. The Cl atom is the dominant oxidant for C ≥ 2 alkanes, while OH is clearly the major player for alkene and aromatic oxidation. The reaction of VOCs and Cl atoms produces additional organic peroxy radicals (RO_2), which are then recycled to hydroperoxyl radicals (HO_2). RO_2 and HO_2 ultimately lead to an increase in O_3 production. By including Cl_2 and $ClNO_2$, the modeled daily RO_2 and HO_2 increased by 18% and 13%, respectively, compared to the scenario that did not have any Cl_2 or $ClNO_2$ input (Figure 5c,d). Over one model day, the integrated O_3 production rate was enhanced by 19% due to increased peroxy radicals. These results imply a significant impact of Cl atoms on peroxy radicals and O_3 production. We also examined VOC ratios for evidence of Cl oxidation (Figure S12).[19,48] Although there are VOC ratios consistent with Cl oxidation, there is a high degree of variability. The VOC ratios do not provide conclusive evidence for Cl oxidation probably because of mixing of air masses from different sources and the dominance of OH as an oxidant.

Our measurements revealed significant levels of Cl_2 and $ClNO_2$ throughout the day on the North China Plain. Since both Cl_2 and $ClNO_2$ photolyze rapidly, the observed levels reflect significant local sources and strong chlorine chemistry. Power plant emissions could be a potential source of Cl_2 precursors. The observation of a reasonable correlation between daytime Cl_2 and $ClNO_2$ implies that both Cl_2 and $ClNO_2$ originate from the same or similar mechanisms. In addition, Cl_2 production is likely associated with a photochemical mechanism as it varied with O_3 levels. Photolysis of the observed Cl_2 and $ClNO_2$ results in Cl atom production, which impact VOC oxidation and radical production. On average, we estimated that the Cl atoms oxidized more alkanes than OH radicals and enhanced the concentrations of peroxy radicals. The enhanced oxidation may result in higher

DOI: 10.1021/acs.est.7b03039
Environ. Sci. Technol. 2017, 51, 9588−9595

O_3 production and thus affect local air quality. To better assess the impact of chlorine chemistry on air quality, further research is needed to explore the distribution of these chlorine species across the NCP region and develop a more thorough understanding of the formation mechanisms of Cl_2 and $ClNO_2$.

■ ASSOCIATED CONTENT

Supporting Information

The Supporting Information is available free of charge on the ACS Publications website at DOI: 10.1021/acs.est.7b03039.

Chlorine chemistry box model and chlorine reactions included, $PM_{2.5}$ pH prediction using ISORROPIA-II and plots of results, summary of Wangdu measurements, relative sensitivities of Cl_2, $ClNO_2$, and PAN as a function of water vapor, correlations of CIMS signals containing chlorine isotopes, example ambient mass spectra, time series of measured chlorine species, wind rose plot of daytime Cl_2, scatter plot of Cl_2 versus $ClNO_2$, average diurnal profiles of model-predicted $ClONO_2$ and simulated $ClNO_2$ and ClONO from Cl + NO_2 reactions, VOC tracer ratios, and time series of Atlanta $ClNO_2$ and Cl_2 measured on January 9, 2013. (PDF)

■ AUTHOR INFORMATION

Corresponding Authors

*E-mail: greg.huey@eas.gatech.edu.
*E-mail: yuhang.wang@eas.gatech.edu.

ORCID

L. Gregory Huey: 0000-0002-0518-7690
Keding Lu: 0000-0001-9425-9520

Notes

The authors declare no competing financial interest.

■ ACKNOWLEDGMENTS

This work was supported by a NSF Grant 1405805. The Peking University team acknowledges support from National Natural Science Foundation of China (21190052, 41421064, and 41375124) and the Strategic Priority Research Program of the Chinese Academy of Sciences (XDB05010500). We thank Hongyu Guo for help with the ISORROPIA-II model. We thank the CAREBEIJING-NCP science team for support during the campaign.

■ REFERENCES

(1) Levy, H. Normal Atmosphere: Large Radical and Formaldehyde Concentrations Predicted. *Science* **1971**, *173* (3992), 141−143.

(2) Crutzen, P. J. Photochemical reactions initiated by and influencing ozone in unpolluted tropospheric air. *Tellus* **1974**, *26* (1−2), 47−57.

(3) Atkinson, R.; Baulch, D. L.; Cox, R. A.; Crowley, J. N.; Hampson, R. F.; Hynes, R. G.; Jenkin, M. E.; Rossi, M. J.; Troe, J.; Subcommittee, I. Evaluated kinetic and photochemical data for atmospheric chemistry: Volume II - gas phase reactions of organic species. *Atmos. Chem. Phys.* **2006**, *6* (11), 3625−4055.

(4) Liao, J.; Huey, L. G.; Liu, Z.; Tanner, D. J.; Cantrell, C. A.; Orlando, J. J.; Flocke, F. M.; Shepson, P. B.; Weinheimer, A. J.; Hall, S. R.; Ullmann, K.; Beine, H. J.; Wang, Y.; Ingall, E. D.; Stephens, C. R.; Hornbrook, R. S.; Apel, E. C.; Riemer, D.; Fried, A.; Mauldin, R. L.; Smith, J. N.; Staebler, R. M.; Neuman, J. A.; Nowak, J. B. High levels of molecular chlorine in the Arctic atmosphere. *Nat. Geosci.* **2014**, *7* (2), 91−94.

(5) Thornton, J. A.; Kercher, J. P.; Riedel, T. P.; Wagner, N. L.; Cozic, J.; Holloway, J. S.; Dubé, W. P.; Wolfe, G. M.; Quinn, P. K.; Middlebrook, A. M.; Alexander, B.; Brown, S. S. A large atomic chlorine source inferred from mid-continental reactive nitrogen chemistry. *Nature* **2010**, *464* (7286), 271−274.

(6) Riedel, T. P.; Bertram, T. H.; Crisp, T. A.; Williams, E. J.; Lerner, B. M.; Vlasenko, A.; Li, S.-M.; Gilman, J.; de Gouw, J.; Bon, D. M.; Wagner, N. L.; Brown, S. S.; Thornton, J. A. Nitryl Chloride and Molecular Chlorine in the Coastal Marine Boundary Layer. *Environ. Sci. Technol.* **2012**, *46* (19), 10463−10470.

(7) Osthoff, H. D.; Roberts, J. M.; Ravishankara, A. R.; Williams, E. J.; Lerner, B. M.; Sommariva, R.; Bates, T. S.; Coffman, D.; Quinn, P. K.; Dibb, J. E.; Stark, H.; Burkholder, J. B.; Talukdar, R. K.; Meagher, J.; Fehsenfeld, F. C.; Brown, S. S. High levels of nitryl chloride in the polluted subtropical marine boundary layer. *Nat. Geosci.* **2008**, *1* (5), 324−328.

(8) Knipping, E. M.; Lakin, M. J.; Foster, K. L.; Jungwirth, P.; Tobias, D. J.; Gerber, R. B.; Dabdub, D.; Finlayson-Pitts, B. J. Experiments and Simulations of Ion-Enhanced Interfacial Chemistry on Aqueous NaCl Aerosols. *Science* **2000**, *288* (5464), 301−306.

(9) Vogt, R.; Crutzen, P. J.; Sander, R. A mechanism for halogen release from sea-salt aerosol in the remote marine boundary layer. *Nature* **1996**, *383* (6598), 327−330.

(10) Oum, K. W.; Lakin, M. J.; DeHaan, D. O.; Brauers, T.; Finlayson-Pitts, B. J. Formation of Molecular Chlorine from the Photolysis of Ozone and Aqueous Sea-Salt Particles. *Science* **1998**, *279* (5347), 74−76.

(11) Sander, R.; Crutzen, P. J. Model study indicating halogen activation and ozone destruction in polluted air masses transported to the sea. *J. Geophys. Res. Atmos.* **1996**, *101* (D4), 9121−9138.

(12) Gebel, M. E.; Finlayson-Pitts, B. J. Uptake and Reaction of $ClONO_2$ on NaCl and Synthetic Sea Salt. *J. Phys. Chem. A* **2001**, *105* (21), 5178−5187.

(13) Tanaka, P. L.; Oldfield, S.; Neece, J. D.; Mullins, C. B.; Allen, D. T. Anthropogenic Sources of Chlorine and Ozone Formation in Urban Atmospheres. *Environ. Sci. Technol.* **2000**, *34* (21), 4470−4473.

(14) Spicer, C. W.; Chapman, E. G.; Finlayson-Pitts, B. J.; Plastridge, R. A.; Hubbe, J. M.; Fast, J. D.; Berkowitz, C. M. Unexpectedly high concentrations of molecular chlorine in coastal air. *Nature* **1998**, *394* (6691), 353−356.

(15) Finley, B. D.; Saltzman, E. S. Measurement of Cl_2 in coastal urban air. *Geophys. Res. Lett.* **2006**, *33* (11), L11809.

(16) Finley, B. D.; Saltzman, E. S. Observations of Cl_2, Br_2, and I_2 in coastal marine air. *J. Geophys. Res.* **2008**, *113* (D21), D21301.

(17) Lawler, M. J.; Sander, R.; Carpenter, L. J.; Lee, J. D.; von Glasow, R.; Sommariva, R.; Saltzman, E. S. HOCl and Cl_2 observations in marine air. *Atmos. Chem. Phys.* **2011**, *11* (15), 7617−7628.

(18) Mielke, L. H.; Furgeson, A.; Osthoff, H. D. Observation of $ClNO_2$ in a Mid-Continental Urban Environment. *Environ. Sci. Technol.* **2011**, *45* (20), 8889−8896.

(19) Baker, A. K.; Sauvage, C.; Thorenz, U. R.; van Velthoven, P.; Oram, D. E.; Zahn, A.; Brenninkmeijer, C. A. M.; Williams, J. Evidence for strong, widespread chlorine radical chemistry associated with pollution outflow from continental Asia. *Sci. Rep.* **2016**, *6*, 36821.

(20) Finlayson-Pitts, B. J.; Ezell, M. J.; Pitts, J. N. Formation of chemically active chlorine compounds by reactions of atmospheric NaCl particles with gaseous N_2O_5 and $ClONO_2$. *Nature* **1989**, *337* (6204), 241−244.

(21) Wang, T.; Tham, Y. J.; Xue, L.; Li, Q.; Zha, Q.; Wang, Z.; Poon, S. C. N.; Dubé, W. P.; Blake, D. R.; Louie, P. K. K.; Luk, C. W. Y.; Tsui, W.; Brown, S. S. Observations of nitryl chloride and modeling its source and effect on ozone in the planetary boundary layer of southern China. *J. Geophys. Res. Atmos.* **2016**, *121* (5), 2476−2489.

(22) Young, C. J.; Washenfelder, R. A.; Roberts, J. M.; Mielke, L. H.; Osthoff, H. D.; Tsai, C.; Pikelnaya, O.; Stutz, J.; Veres, P. R.; Cochran, A. K.; VandenBoer, T. C.; Flynn, J.; Grossberg, N.; Haman, C. L.; Lefer, B.; Stark, H.; Graus, M.; de Gouw, J.; Gilman, J. B.; Kuster, W. C.; Brown, S. S. Vertically Resolved Measurements of Nighttime Radical Reservoirs in Los Angeles and Their Contribution to the Urban Radical Budget. *Environ. Sci. Technol.* **2012**, *46* (20), 10965−10973.

(23) Riedel, T. P.; Wolfe, G. M.; Danas, K. T.; Gilman, J. B.; Kuster, W. C.; Bon, D. M.; Vlasenko, A.; Li, S. M.; Williams, E. J.; Lerner, B. M.;

DOI: 10.1021/acs.est.7b03039
Environ. Sci. Technol. 2017, 51, 9588−9595

Veres, P. R.; Roberts, J. M.; Holloway, J. S.; Lefer, B.; Brown, S. S.; Thornton, J. A. An MCM modeling study of nitryl chloride ($ClNO_2$) impacts on oxidation, ozone production and nitrogen oxide partitioning in polluted continental outflow. *Atmos. Chem. Phys.* **2014**, *14* (8), 3789−3800.
(24) Tao, M.; Chen, L.; Su, L.; Tao, J. Satellite observation of regional haze pollution over the North China Plain. *J. Geophys. Res. Atmos.* **2012**, *117* (D12), D12203.
(25) Ma, J.; Chen, Y.; Wang, W.; Yan, P.; Liu, H.; Yang, S.; Hu, Z.; Lelieveld, J. Strong air pollution causes widespread haze-clouds over China. *J. Geophys. Res.* **2010**, *115* (D18), D18204.
(26) Tham, Y. J.; Wang, Z.; Li, Q.; Yun, H.; Wang, W.; Wang, X.; Xue, L.; Lu, K.; Ma, N.; Bohn, B.; Li, X.; Kecorius, S.; Größ, J.; Shao, M.; Wiedensohler, A.; Zhang, Y.; Wang, T. Significant concentrations of nitryl chloride sustained in the morning: investigations of the causes and impacts on ozone production in a polluted region of northern China. *Atmos. Chem. Phys.* **2016**, *16* (23), 14959−14977.
(27) Liu, P.; Zhang, C.; Xue, C.; Mu, Y.; Liu, J.; Zhang, Y.; Tian, D.; Ye, C.; Zhang, H.; Guan, J. The contribution of residential coal combustion to atmospheric $PM_{2.5}$ in the North China during winter. *Atmos. Chem. Phys. Discuss.* **2017**, *2017*, 1−37.
(28) Slusher, D. L.; Huey, L. G.; Tanner, D. J.; Flocke, F. M.; Roberts, J. M. A thermal dissociation−chemical ionization mass spectrometry (TD-CIMS) technique for the simultaneous measurement of peroxyacyl nitrates and dinitrogen pentoxide. *J. Geophys. Res.* **2004**, *109* (D19), D19315.
(29) Liao, J.; Sihler, H.; Huey, L. G.; Neuman, J. A.; Tanner, D. J.; Friess, U.; Platt, U.; Flocke, F. M.; Orlando, J. J.; Shepson, P. B.; Beine, H. J.; Weinheimer, A. J.; Sjostedt, S. J.; Nowak, J. B.; Knapp, D. J.; Staebler, R. M.; Zheng, W.; Sander, R.; Hall, S. R.; Ullmann, K. A comparison of Arctic BrO measurements by chemical ionization mass spectrometry and long path-differential optical absorption spectroscopy. *J. Geophys. Res.* **2011**, *116* (D14), D00r02.
(30) Warneck, P.; Zerbach, T. Synthesis of peroxyacetyl nitrate in air by acetone photolysis. *Environ. Sci. Technol.* **1992**, *26* (1), 74−79.
(31) Thaler, R. D.; Mielke, L. H.; Osthoff, H. D. Quantification of nitryl chloride at part per trillion mixing ratios by thermal dissociation cavity ring-down spectroscopy. *Anal. Chem.* **2011**, *83* (7), 2761−6.
(32) Kebabian, P. L.; Wood, E. C.; Herndon, S. C.; Freedman, A. A Practical Alternative to Chemiluminescence-Based Detection of Nitrogen Dioxide: Cavity Attenuated Phase Shift Spectroscopy. *Environ. Sci. Technol.* **2008**, *42* (16), 6040−6045.
(33) De Laeter, J. R.; Böhlke, J. K.; De Bièvre, P.; Hidaka, H.; Peiser, H. S.; Rosman, K. J. R.; Taylor, P. D. P. Atomic weights of the elements: Review 2000 (IUPAC Technical Report). *Pure Appl. Chem.* **2003**, *75* (6), 683−800.
(34) Volpe, C.; Wahlen, M.; Pszenny, A. A. P.; Spivack, A. J. Chlorine isotopic composition of marine aerosols: Implications for the release of reactive chlorine and HCl cycling rates. *Geophys. Res. Lett.* **1998**, *25* (20), 3831−3834.
(35) Koehler, G.; Wassenaar, L. I. The stable isotopic composition ($^{37}Cl/^{35}Cl$) of dissolved chloride in rainwater. *Appl. Geochem.* **2010**, *25* (1), 91−96.
(36) Wang, Y.; Choi, Y.; Zeng, T.; Davis, D.; Buhr, M.; Gregory Huey, L.; Neff, W. Assessing the photochemical impact of snow NO_x emissions over Antarctica during ANTCI 2003. *Atmos. Environ.* **2007**, *41* (19), 3944−3958.
(37) Zhang, Y.; Wang, Y.; Chen, G.; Smeltzer, C.; Crawford, J.; Olson, J.; Szykman, J.; Weinheimer, A. J.; Knapp, D. J.; Montzka, D. D.; Wisthaler, A.; Mikoviny, T.; Fried, A.; Diskin, G. Large Vertical Gradient of Reactive Nitrogen Oxides in the Boundary Layer: Modeling Analysis of DISCOVER-AQ 2011 Observations. *J. Geophys. Res. Atmos.* **2016**, *121* (4), 1922−1934.
(38) Liu, Z.; Wang, Y.; Gu, D.; Zhao, C.; Huey, L. G.; Stickel, R.; Liao, J.; Shao, M.; Zhu, T.; Zeng, L.; Liu, S.-C.; Chang, C.-C.; Amoroso, A.; Costabile, F. Evidence of Reactive Aromatics As a Major Source of Peroxy Acetyl Nitrate over China. *Environ. Sci. Technol.* **2010**, *44* (18), 7017−7022.
(39) Bannan, T. J.; Booth, A. M.; Bacak, A.; Muller, J. B. A.; Leather, K. E.; Le Breton, M.; Jones, B.; Young, D.; Coe, H.; Allan, J.; Visser, S.; Slowik, J. G.; Furger, M.; Prévôt, A. S. H.; Lee, J.; Dunmore, R. E.; Hopkins, J. R.; Hamilton, J. F.; Lewis, A. C.; Whalley, L. K.; Sharp, T.; Stone, D.; Heard, D. E.; Fleming, Z. L.; Leigh, R.; Shallcross, D. E.; Percival, C. J. The first UK measurements of nitryl chloride using a chemical ionization mass spectrometer in central London in the summer of 2012, and an investigation of the role of Cl atom oxidation. *J. Geophys. Res. Atmos.* **2015**, *120* (11), 5638−5657.
(40) Faxon, B. C.; Bean, K. J.; Ruiz, H. L. Inland Concentrations of Cl_2 and $ClNO_2$ in Southeast Texas Suggest Chlorine Chemistry Significantly Contributes to Atmospheric Reactivity. *Atmosphere* **2015**, *6* (10), 1487−1506.
(41) Zhao, Y.; Wang, S.; Duan, L.; Lei, Y.; Cao, P.; Hao, J. Primary air pollutant emissions of coal-fired power plants in China: Current status and future prediction. *Atmos. Environ.* **2008**, *42* (36), 8442−8452.
(42) Tan, Z.; Fuchs, H.; Lu, K.; Bohn, B.; Broch, S.; Dong, H.; Gomm, S.; Haeseler, R.; He, L.; Hofzumahaus, A.; Holland, F.; Li, X.; Liu, Y.; Lu, S.; Rohrer, F.; Shao, M.; Wang, B.; Wang, M.; Wu, Y.; Zeng, L.; Zhang, Y.; Wahner, A.; Zhang, Y. Radical chemistry at a rural site (Wangdu) in the North China Plain: observation and model calculations of OH, HO_2 and RO_2 radicals. *Atmos. Chem. Phys.* **2017**, *17*, 663−690.
(43) Roberts, J. M.; Osthoff, H. D.; Brown, S. S.; Ravishankara, A. R. N_2O_5 Oxidizes Chloride to Cl_2 in Acidic Atmospheric Aerosol. *Science* **2008**, *321* (5892), 1059.
(44) Nenes, A.; Pandis, S. N.; Pilinis, C. ISORROPIA: A New Thermodynamic Equilibrium Model for Multiphase Multicomponent Inorganic Aerosols. *Aquat. Geochem.* **1998**, *4* (1), 123−152.
(45) Fountoukis, C.; Nenes, A. ISORROPIA II: a computationally efficient thermodynamic equilibrium model for K^+-Ca^{2+}-Mg^{2+}-NH_4^+-Na^+-SO_4^{2-}-NO_3^--Cl^--H_2O aerosols. *Atmos. Chem. Phys.* **2007**, *7* (17), 4639−4659.
(46) Keene, W. C.; Pszenny, A. A. P.; Maben, J. R.; Stevenson, E.; Wall, A. Closure evaluation of size-resolved aerosol pH in the New England coastal atmosphere during summer. *J. Geophys. Res. Atmos.* **2004**, *109* (D23), D23307.
(47) Yao, X.; Ling, T. Y.; Fang, M.; Chan, C. K. Size dependence of in situ pH in submicron atmospheric particles in Hong Kong. *Atmos. Environ.* **2007**, *41* (2), 382−393.
(48) Young, C. J.; Washenfelder, R. A.; Edwards, P. M.; Parrish, D. D.; Gilman, J. B.; Kuster, W. C.; Mielke, L. H.; Osthoff, H. D.; Tsai, C.; Pikelnaya, O.; Stutz, J.; Veres, P. R.; Roberts, J. M.; Griffith, S.; Dusanter, S.; Stevens, P. S.; Flynn, J.; Grossberg, N.; Lefer, B.; Holloway, J. S.; Peischl, J.; Ryerson, T. B.; Atlas, E. L.; Blake, D. R.; Brown, S. S. Chlorine as a primary radical: evaluation of methods to understand its role in initiation of oxidative cycles. *Atmos. Chem. Phys.* **2014**, *14* (7), 3427−3440.

DOI: 10.1021/acs.est.7b03039
Environ. Sci. Technol. 2017, 51, 9588−9595